Available online at www.sciencedirect.com
SCIENCE DIRECT®
Journal of Catalysis 237 (2006) 102–110
JOURNAL OF CATALYSIS
www.elsevier.com/locate/jcat

Pulse-response TAP studies of the reverse water–gas shift reaction over a Pt/CeO_2 catalyst

A. Goguet [a], S.O. Shekhtman [a], R. Burch [a], C. Hardacre [a,*], F.C. Meunier [a], G.S. Yablonsky [b]

[a] *CenTACat, School of Chemistry and Chemical Engineering, Queen's University Belfast, Belfast BT9 5AG, Northern Ireland, UK*
[b] *Washington University, Department of Chemical Engineering, St Louis, MO 63130, USA*

Received 12 September 2005; revised 14 October 2005; accepted 17 October 2005

Available online 28 November 2005

Abstract

The temporal analysis of products (TAP) technique was successfully applied for the first time to investigate the reverse water–gas shift (RWGS) reaction over a 2% Pt/CeO_2 catalyst. The adsorption/desorption rate constants for CO_2 and H_2 were determined in separate TAP pulse-response experiments, and the number of H-containing exchangeable species was determined using D_2 multipulse TAP experiments. This number is similar to the amount of active sites observed in previous SSITKA experiments. The CO production in the RWGS reaction was studied in a TAP experiment using separate (sequential) and simultaneous pulsing of CO_2 and H_2. A small yield of CO was observed when CO_2 was pulsed alone over the reduced catalyst, whereas a much higher CO yield was observed when CO_2 and H_2 were pulsed consecutively. The maximum CO yield was observed when the CO_2 pulse was followed by a H_2 pulse with only a short (1 s) delay. Based on these findings, we conclude that an associative reaction mechanism dominates the RWGS reaction under these experimental conditions. The rate constants for several elementary steps can be determined from the TAP data. In addition, using a difference in the time scale of the separate reaction steps identified in the TAP experiments, it is possible to distinguish a number of possible reaction pathways.
© 2005 Elsevier Inc. All rights reserved.

Keywords: Temporal analysis of products; Ceria; Water–gas shift; Pt

1. Introduction

The water–gas shift (WGS) reaction is a key step in applications such as H_2 production via reforming processes for fuel cell applications, particularly for mobile sources. In such applications, a successful low-temperature WGS catalyst must retain high activity and structural stability over a wide range of reaction conditions, including both gas composition and temperature. To date, although a number of highly active catalysts have been reported, the catalysts often deactivate with temperature, in particular. The importance of this process is exemplified by the numerous research programs aimed at discovering more stable high-activity catalysts. In this regard, the activity of platinum group metals (PGM) supported on rare earth oxides as catalysts to promote the WGS reaction has attracted much attention, with ceria-supported catalysts in particular showing similar or higher activity than the more conventional $Cu/ZnO/Al_2O_3$ materials under some reaction conditions [1–19]. However, the activity and stability of ceria-based formulations depends markedly on the preparation method used [8,20–24]. Therefore, there is a need for a better understanding of the reaction mechanism over these types of catalysts, to enable further improvement in their formulation and preparation.

To date, two main reaction mechanisms have been proposed: a redox process (Scheme 1) and an associative "formate" mechanism (Scheme 2). In the redox mechanism, CO adsorbs on reduced metal sites and reacts with an oxygen atom coming from

$$Pt + CO \leftrightarrow Pt\text{–}CO, \quad \text{(I)}$$

$$Pt\text{–}CO + 2CeO_2 \leftrightarrow CO_2 + Ce_2O_3 + Pt, \quad \text{(II)}$$

$$H_2O + Ce_2O_3 \leftrightarrow 2CeO_2 + H_2. \quad \text{(III)}$$

Scheme 1.

* Corresponding author. Fax: +44 (0) 28 9097 4687.
E-mail address: c.hardacre@qub.ac.uk (C. Hardacre).

0021-9517/$ – see front matter © 2005 Elsevier Inc. All rights reserved.
doi:10.1016/j.jcat.2005.10.020

$$CO + \sigma \leftrightarrow CO_{ad}, \quad \text{(I)}$$

$$H_2O + 2\sigma \leftrightarrow H_{ad} + OH_{ad}, \quad \text{(II)}$$

$$CO_{ad} + OH_{ad} \leftrightarrow HCOO_{ad} + \sigma, \quad \text{(III)}$$

$$HCOO_{ad} + \sigma \leftrightarrow CO_{2,ad} + H_{ad}, \quad \text{(IV)}$$

$$CO_{2,ad} \leftrightarrow CO_2 + \sigma, \quad \text{(V)}$$

$$2H_{ad} \leftrightarrow H_2 + 2\sigma. \quad \text{(VI)}$$

Scheme 2.

the ceria to form CO_2. The reduced ceria is subsequently reoxidized by water, releasing hydrogen [8,10,20,21,25]. In the associative mechanism, the main reaction intermediate is a bidentate formate, produced by reaction of CO with terminal hydroxyl groups on the oxide support, which decomposes to form H_2 and a monodentate carbonate [3,26–31]. In Scheme 2, σ refers to sites on the oxide support.

Along with whether a redox or an associative reaction mechanism is responsible for the WGS activity over oxide-supported PGM catalysts, the role of the PGM in the surface reaction has also been addressed. Flytzani–Stephanopoulos and coworkers recently reported that on removal of all transmission electron microscopy (TEM)-observable PGM particles, the activity of ceria-supported gold and platinum catalysts remained unchanged compared with that of the as-prepared catalysts [32–34]. These authors proposed that active metal, in the form of cations, diffuses into the ceria and is anchored at surface defects. These ions increase the reducibility of the support, with any remaining zerovalent metal considered unimportant in the WGS reaction. This mechanism is a modification of the normal-support activation (NSA) effect summarized by Golunski et al. [35] and originally proposed by Frost [36] for methanol synthesis catalysts. This junction effect modification between the PGM and oxide support leads to a dramatic increase in the number of oxygen vacancies within the support, which become the active sites—a reversal of the conventional roles of the oxide and the PGM.

This may be contrasted with a recent in situ EXAFS and DFT study on similar catalysts demonstrating that the state of the catalyst under reaction conditions may be significantly different than that of the prepared catalyst [37]. Although $Au/CeZrO_4$ catalysts exhibit cationic gold in the fresh catalyst, under mild WGS reaction conditions, rapid reduction of the gold and agglomeration into 1- to 2-nm particles occurred. The EXAFS and XANES experimental results combined with DFT calculations point to a model in which a metallic gold cluster containing about 50 atoms is in intimate contact with the oxide support to the extent that up to 15% of the gold "atoms" at the interface with the support may be located at cation vacancies. Such gold atoms would be expected to carry a small positive charge ($Au^{\delta+}$), which may be very important in creating the active site for the WGS reaction. However, it is clear that for these catalysts, metallic gold particles, not isolated gold ions (e.g., Au^{3+}), are present under reaction conditions [37]. Similarly, there is strong evidence for involvement of the support in the RWGS reaction mechanism over Pt/CeO_2 catalysts [38]. It has been proposed that during the reaction, a limited fraction of the support close to the metal particles could be in a partially reduced state and would correspond to the active part of the support.

The reaction mechanism is further complicated by the fact that the surface composition, and thus the main reaction steps, can dramatically depend on the experimental procedure used during the reaction. Based on DRIFTS analysis combined with the use of isotopic tracers, formates were found to be less labile than carbonyl and carbonate species under steady-state reaction conditions over a 2% Pt/CeO_2 catalyst, whereas the carbonates were found to be most stable during the desorption-type non-steady-state experiments carried out in an inert purge gas [39]. Furthermore, combining mass spectrometry and DRIFTS analysis during SSITKA experiments under operating conditions over a Pt/CeO_2 catalyst showed that it was possible to discard formate species as a major reaction intermediate under RWGS reaction conditions [40,41]. Quantification of the number of active sites showed that the Pt-carbonyl species could not be the only reaction intermediates and that for this catalyst under these conditions, the RWGS reaction proceeds via surface carbonate intermediates, possibly followed by the formation of Pt-bound carbonyls. In this reaction mechanism, the direct reoxidation of the support by the CO_2 is proposed, and the active sites involved in this reaction step are distributed as a circular zone around the Pt particles.

Although much less studied than steady-state reaction data, non-steady-state kinetic information has proven to be a powerful tool in revealing the detailed mechanism and roles of different surface intermediates for a wide range of catalytic reactions including the WGS process [10,13]. For example, Gorte and Zhao used normal pressure-pulse studies to observe the reaction steps in the proposed redox mechanism for WGS over Pd/CeO_2 catalyst [25]. Therein, the catalyst was repeatedly exposed to two 250-s CO pulses followed by two H_2O pulses. Both the initial pulses of CO and H_2O led to production CO_2 and H_2, with the H_2 thought to originate from the decomposition of surface hydroxyls and the CO_2 from removal of surface carbonates. Consequently, reactions between the pulsed gas reactants and surface intermediates must occur to explain these non-steady-state kinetic data. Although this study provides insight into the reaction mechanism, at normal pressures the surface composition is not generally well defined, and it changes significantly during each pulse. This is clearly shown by the large change in response to CO and H_2O after the first and second pulses of each gas. This changing surface state hinders interpretation and quantification of the non-steady-state normal pressure data.

Over the last two decades, the temporal analysis of products (TAP) technique, developed by Gleaves and co-workers [42,43], has been successfully applied to non-steady-state kinetic characterization of model and multicomponent industrial catalysts in many areas of chemical kinetics and engineering [44]. The technique provides an opportunity to control the catalyst composition so that it does not change significantly during a single-pulse experiment, but can be changed in a controlled manner in a long trail of low-intensity pulses [45].

This paper demonstrates for the first time that the TAP technique can be applied to the RWGS reaction to provide unique

information on the nature and reactivity of key surface intermediates that may be relevant to the reaction mechanism for a 2% Pt/CeO_2 catalyst. The reaction between the specific gas reactants and a catalyst that has been conditioned to have a particular surface composition was measured to identify the separate elementary steps of the reaction mechanism.

2. Experimental

The catalyst used in this study was a 2% Pt/CeO_2 provided by Johnson Matthey. The specific surface area was measured by BET (Micromeretics ASAP 2010) and was found to be 180 $m^2\,g^{-1}$. The Pt dispersion was measured by H_2 chemisorption (Micromeretics Autochem 2910) and was found to be 17%. Note that the dispersion measurements were performed at −80 °C to minimize the potential spillover of H_2 onto the support [46]. For all of the experiments described below, the gases (H_2, Ar, CO, and CO_2) were of >99.9% purity, supplied by BOC. Before each reaction, the catalyst was activated under flowing 20% oxygen in nitrogen for 1 h, followed by reduction in pure hydrogen for 1 h at 300 °C and 1 atm pressure. In addition, CO_2 pretreatment after the oxidation-reduction cycle was performed at 300 °C and 1 atm pressure using flowing pure CO_2 for 1 h.

The TAP pulse-response experiments were performed in a TAP-I reactor (Autoclave Engineers) using a stainless steel microreactor (41 mm long, 5.5 mm i.d.). In all experiments, the thin-zone TAP reactor (TZTR) concept developed by Shekhtman and Yablonsky was used, where uniformity of gas and surface concentration in the catalyst zone is achieved by making the active zone thin compared with the length of the reactor [47]. In the TZTR, diffusion dampens the nonuniformity in the concentration created by reaction to 15–20% over a wide domain of conversions (up to 80%) [48–50]. Another key feature of the TZTR is that the gas concentration in the catalyst zone can be approximated as being proportional to the observed responses, which allows the correlation of the product response with those associated with the reactants. The details of this approximation will be reported elsewhere [51].

The TZTR was packed with two 17-mm-long beds of silicon carbide sandwiching 1 mm of catalyst. All particles were 250–450 μm in size. The temperature of the reactor was measured by a thermocouple positioned in the center of the catalyst bed. Reactants and products were recorded at the reactor outlet by a UTI 100C quadrupole mass spectrometer. The temperature was kept constant during the normal pressure treatment and vacuum pulse response experiments at 300 °C. The response collection time was 15 s. In all experiments, reactant pulses were diluted by argon in a ratio of 1:1, and masses characteristic of all reactants and possible products (CO, CO_2, H_2, CH_4, and H_2O) were followed. The following procedure was used for all experiments:

1. Pretreatment of the catalyst by exposing to different gases at 1 atm pressure.
2. Evacuation of the reactor to 10^{-6} Torr.
3. Vacuum pulse-response TAP experiments using (i) single reactant pulses, (ii) simultaneously pulsing two reagents, or (iii) pulsing two reagents with a time delay.

The exit flow-rate time dependence for reactants and products was extracted from the mass spectrometer data using standard fragmentation patterns and sensitivity factors normalized to the inert (argon).

In the Knudsen diffusion flow regime, the product pulse shape is independent of the pulse intensity [42]. Therefore, to maintain the Knudsen conditions and to avoid altering the catalyst state on pulsing, the number of reactant molecules in each TAP pulse was only $\sim 7 \times 10^{-9}$ mol. This may be compared with an estimate of 3×10^{-6} mol for the amount of active intermediates or oxygen on the catalyst surface from the CO/CO_2 released by the sample in a SSITKA experiment [40]. Thus, a large number of reactant pulses are required to change the catalyst composition significantly.

3. Results and discussion

3.1. CO_2 adsorption

The interaction of CO_2 with the catalysts as a function of the pretreatment was studied by consecutive pulsing of CO_2 over the Pt/CeO_2 catalyst. The following observations were made (Fig. 1):

1. Over the reduced and CO_2 pretreated catalyst, fast reversible adsorption mainly on ceria sites was found, resulting in broad peak responses. Fig. 1 shows a typical CO_2 response.
2. Very small amounts of CO were produced.
3. Not all injected CO_2 molecules were observed at the outlet of the reactor in the single-pulse experiment.
4. No significant change of CO_2 responses was observed when the pretreated catalysts were exposed to a large number of CO_2 pulses (up to 10,000) in a multipulse experiment, irrespective of the pretreatment.

Observation 3 indicates that CO_2 forms surface intermediates that do not decompose within the time scale of the single-pulse experiment, which is 15 s. It is clear from observation 4

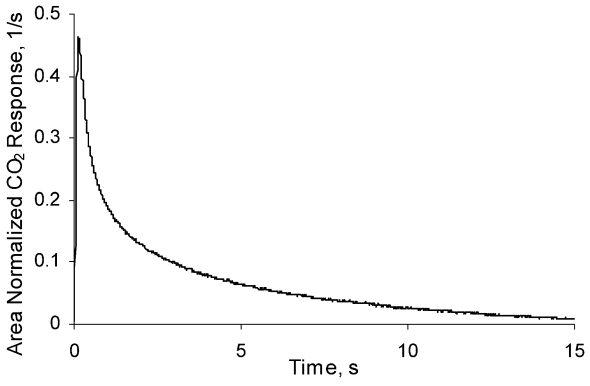

Fig. 1. A typical broad CO_2 response over the 2% Pt/CeO_2 catalyst at 300 °C.

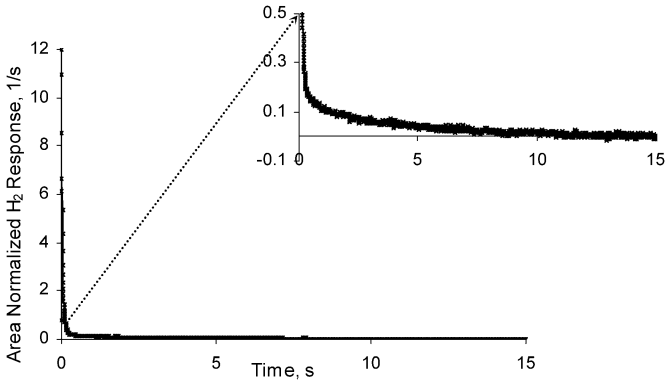

Fig. 2. A typical H_2 response over the 2% Pt/CeO_2 catalyst at 300 °C. The broad tail is plotted on a magnified scale.

that these intermediates are desorbed, and hence they do not accumulate on the catalyst. It was not possible to completely saturate the surface even after thousands of CO_2 pulses over hours. Given the relative time scales for the TAP experiments and the delay between pulses, it can be concluded that these surface intermediates decompose on the minute time scale, that is, faster than the timescale of the multipulse TAP experiments but slower than the time scale of the single-pulse TAP experiment. Such decomposition contributes to the baseline and cannot be monitored as a pulse response.

Analysis of the reversible fast interaction of CO_2 with the catalyst from a single-pulse response TAP experiment shows that it may be described in terms of apparent adsorption and desorption rate constants, $k_a = 170\ s^{-1}$ and $k_d = 1.3\ s^{-1}$, respectively.

3.2. Hydrogen adsorption

The following were observed for H_2 pulsed over the reduced or CO_2-treated Pt/CeO_2 catalyst (see Fig. 2):

1. Fast reversible adsorption on the catalyst, resulting in a sharp peak (due to fast H_2 diffusion) and a long tail, as shown in Fig. 2.
2. Little change in the H_2 responses as a function of pulse number in multipulse experiments, indicating a reversible interaction of H_2 with the catalyst.

As was found for CO_2, the reversible interaction of H_2 with the catalyst observed in a TAP experiment can be described in terms of an apparent adsorption and desorption rate constant, $k_a = 110\ s^{-1}$ and $k_d = 0.9\ s^{-1}$, respectively.

To probe the dissociative adsorption and desorption process for the hydrogen, deuterium was pulsed over a hydrogen-treated catalyst and the responses for D_2, DH, and H_2 were monitored. As shown in Fig. 3a, the intensity of the D_2 responses increases with pulse number, whereas the intensity of the DH and H_2 responses decrease indicating a decrease in the of amount of surface hydrogen available for the D–H exchange with each progressive pulse of D_2. The total amount of D_2 molecules that underwent D–H exchange in this experiment was estimated as $3 \times 10^{-4}\ mol\, g_{cat}^{-1}$. This number can be associated

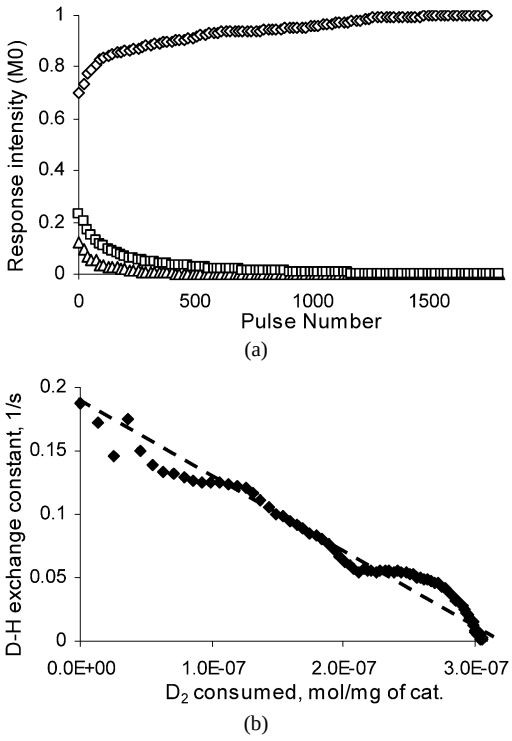

Fig. 3. (a) H_2 (△), DH (□) and D_2 (◇) response intensities versus pulse number and (b) D–H exchange rate constant versus the amount of D_2 consumed observed following deuterium pulsing over hydrogen treated 2% Pt/CeO_2 catalyst.

with the amount of H-containing species located on or around the platinum particle. Remarkably, this number agrees very well with the amount of exchangeable sites observed with a SSITKA experiment using isotopically labeled carbon molecules ($2.2 \times 10^{-4}\ mol\, g^{-1}$) [40], which may indicate that the active intermediate or transient state complex contains both carbon and hydrogen.

Fig. 3b shows how the rate constant for surface D–H exchange varies as a function of the amount of D_2 exchanged. A clear linear trend is found indicating a first-order kinetic dependence with respect to H-containing active species.

3.3. Pulsing of CO_2 and H_2

Over a preoxidized and then prereduced catalyst, $^{13}CO_2$ and H_2 were pulsed simultaneously or with an increasing time delay between the reactants; the latter sequence is illustrated in Fig. 4. The results of these experiments compared with those with $^{13}CO_2$ and H_2 pulsed separately are shown in Fig. 5. As described above, when CO_2 was pulsed alone, only a small yield of CO (<0.5%) was observed. It should be noted that this was only quantifiable using $^{13}CO_2$, due to the increased sensitivity of the 29-amu signal compared with the 28-amu signal, which is masked to a degree by the background gas signal. As expected, no CO was observed on pulsing hydrogen alone. However, when $^{13}CO_2$ was repeatedly pulsed followed by the hydrogen pulse with different time delays, (i.e., consecutive pulsing), the observed CO yield was significantly higher and decreased with increasing time delay. The CO response profiles

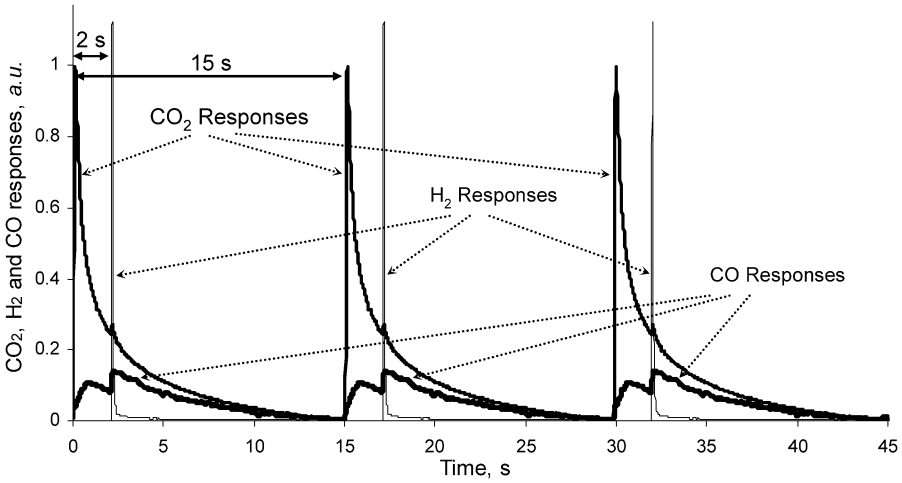

Fig. 4. $^{13}CO_2$, H_2 and ^{13}CO responses observed in the consecutive pulsing TAP experiment using a collection time of 15 s with a time delay of 2 s between the $^{13}CO_2$ and H_2 pulses.

showed a sharp increase in CO production coincident with the hydrogen pulse and superimposed on a broad CO peak with a slowly decaying tail.

The broad CO_2 responses indicate that CO_2 was present in the catalyst zone during most of the 15-s time interval, with a maximum at approximately 0.13 s after the pulse. According to the hydrogen response, the concentration of hydrogen in the catalyst zone sharply increased once it was pulsed, then dropped quickly by more than an order of magnitude, as shown in Fig. 4. No significant change in hydrogen response was observed with time delay. According to the CO responses, the amount of CO produced increases sharply after the hydrogen response and decays slowly thereafter. This may indicate that H_2 quickly adsorbs and reacts with a surface intermediate that then subsequently releases CO. This behavior is not observed when $^{13}CO_2$ and H_2 are pulsed simultaneously, in which case the CO response does not rise sharply but reaches a maximum at 0.63 s after the pulses, later than the maximum reached by either the H_2 or CO_2. This indicates that the CO_2 reacts to form an active surface intermediate on a time scale of seconds.

The CO responses may be deconvoluted into two peaks for CO production. The position of the first peak, shown by the arrow in Fig. 5b, does not change with the H_2 pulse time delay, with a maximum occurring after 0.6–1.0 s. A small decrease is observed in the intensity of the peak with increasing time delay of the H_2. The sharp second peak closely follows the time of the H_2 pulse, the intensity of which monotonously decreases with increasing time delay.

The constant position and broad front of the first peak are consistent with a relatively slow reaction between CO_2 pulsed at $t = 0$ s and a catalyst surface with some coverage of adsorbed hydrogen. The decreasing intensity with increasing time delay of the H_2 reflects the fact that the adsorbed hydrogen must transform into an active species before it can react with the CO_2 pulse. As this takes a finite amount of time, and an increasing time delay between the CO_2 pulse and the next H_2 pulse results in a *decreasing* time delay between the H_2 pulse and the next CO_2 pulse, the concentration of active hydrogen decreases leading to the lower CO yield at $t = 0$ s. Remarkably, it takes around 1 s to produce CO. In comparison, the sharp leading edge of the second peak corresponds to a relatively fast reaction between pulsed H_2 and a catalyst surface with adsorbed CO_2 intermediates.

Preliminary CO multipulse experiments have shown that CO desorption is fast, with a desorption rate constant $k_d \approx 1.5\ s^{-1}$, and hence the reactions are not CO desorption rate limited at this temperature. The sharp increase in CO yield after the H_2 pulse may reflect the absence of limiting steps within this pathway. Thus, the rate of slow CO release must be limited by the formation of the CO_2-containing surface intermediate. The logarithmic plot of CO responses with respect to time shown in Fig. 6 indicate that the decrease in CO production after each of the two peaks is governed by a common exponential decay constant, $k_{exp} = 0.2\ s^{-1}$, which can be explained by decomposition of the same intermediate, that is, whether the reaction is initiated by the CO_2 pulse or the H_2 pulse. However, there is a significant difference in the time for formation of this intermediate and hence the broad and sharp response on CO_2 and H_2 pulsing, respectively. This may be indicative of the higher rate of surface diffusion and reduced adsorption strength of H_2 compared with CO_2 over the catalyst.

Fig. 7a shows the CO/CO_2 response intensities normalized to argon versus the H_2 pulse time delay. The plot also shows partial contributions to the CO response from the time intervals after the hydrogen pulse. The intensity of the CO_2 response decreases with increasing time delay, reflecting the influence of the H_2 pulse on the CO_2–catalyst interaction. In these vacuum pulse response TAP experiments, the observed CO yield is $<4\%$, and it exhibits a maximum at 1 s delay of the hydrogen pulse, then decreases with increasing time delay. This decrease is associated with the reduced CO production after the hydrogen pulse and may be associated with the amount of intermediate available for a fast reaction with adsorbed hydrogen. Fig. 7b shows a logarithmic plot of the CO yield after the hydrogen pulse, which exhibits an exponential decay with a rate constant $k \approx 0.24\ s^{-1}$. This decay can be attributed to decomposition of the active CO_2-containing intermediate with which adsorbed H_2 reacts. As the time delay for the hydrogen increases beyond

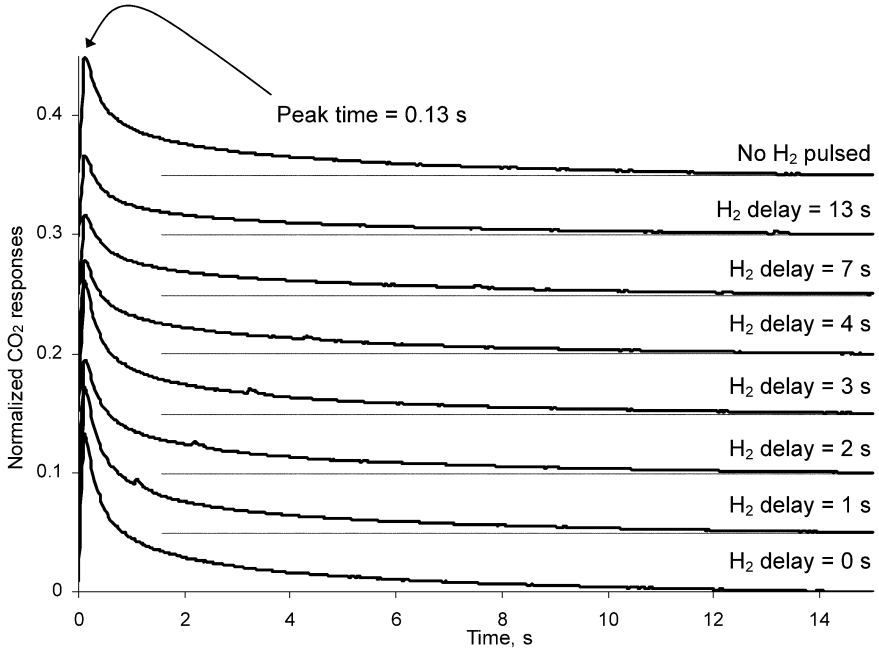

(a)

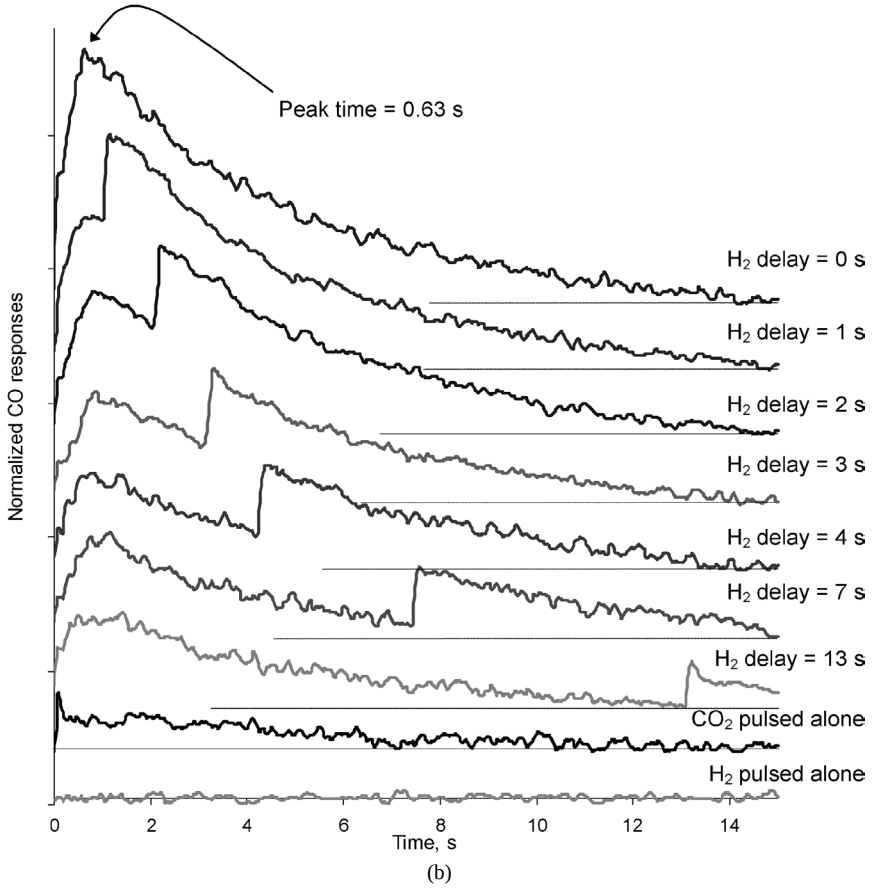

(b)

Fig. 5. (a) $^{13}CO_2$ and (b) ^{13}CO responses observed when $^{13}CO_2$ and H_2 were pulsed alone or consecutively with different time delays for H_2, in each case the $^{13}CO_2$ is pulsed at 0 s and the H_2 is pulsed after the corresponding time delay. The dotted lines define the base lines for the corresponding $^{13}CO_2$ and ^{13}CO responses.

2 s, the surface concentration of this intermediate drops and hence the CO yield decreases.

The fact that a small CO yield (<0.5%) is observed when CO_2 is pulsed alone over reduced catalyst compared with the CO yield (up to 3.5%) in consecutive pulsing (Fig. 5b) clearly proves that the presence of both reactants is critical for CO production. Thus, under the TAP conditions used herein, an associative mechanism is primarily operating for the RWGS re-

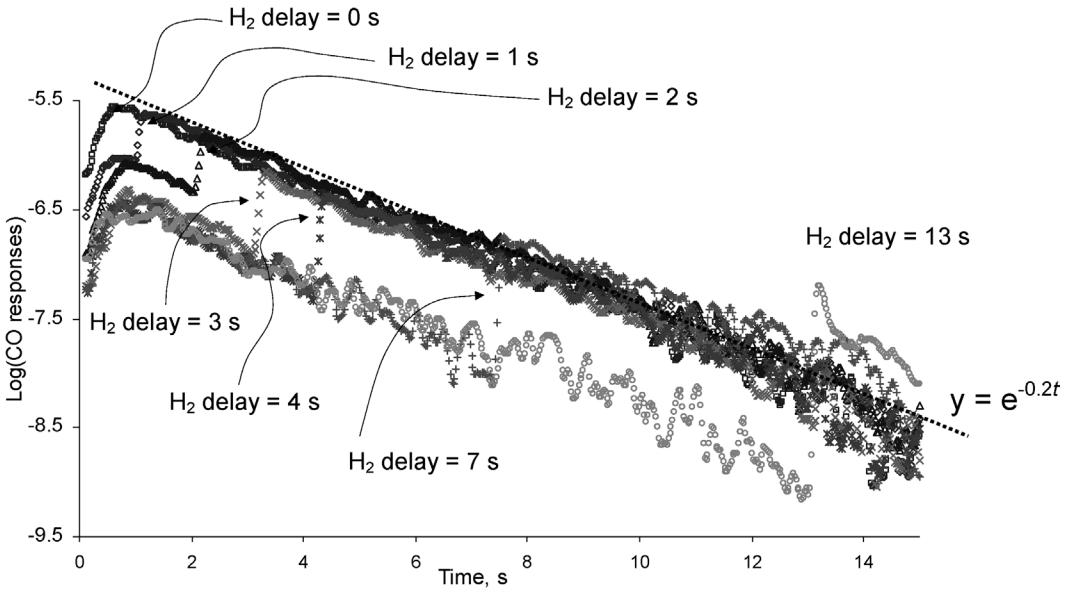

Fig. 6. ^{13}CO responses versus time observed when $^{13}CO_2$ and H_2 were pulsed consecutively with different H_2 time delays plotted on the logarithmic scale. The dashed line shows the exponential fitting of the decay curve, $y = e^{-0.2t}$.

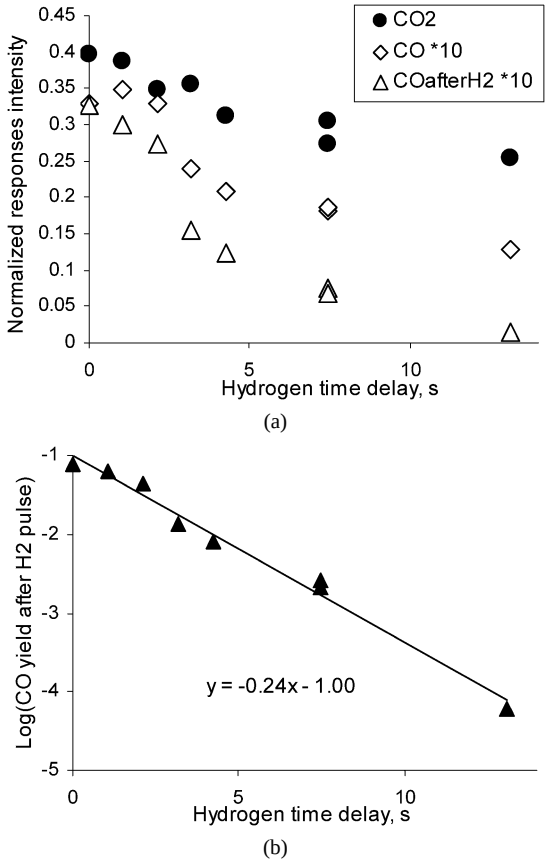

Fig. 7. (a) Normalized response intensities for total $^{13}CO_2$ (●), total $^{13}CO \times 10$ (◇) production and ^{13}CO production measured after hydrogen pulse $\times 10$ (△) versus the H_2 pulse time delay and (b) ^{13}CO yield after hydrogen pulse plotted on a logarithmic scale versus the time delay.

action. Scheme 3 shows a tentative reaction mechanism for the fast reaction observed under TAP conditions.

Step (I) reflects the fast adsorption/desorption observed for CO_2. Here σ is an adsorption site for CO_2, probably associated primarily with the ceria support. Step (II) reflects the fast adsorption/desorption observed for H_2, most likely associated with the metal sites. Step (III) describes the formation of a specific C-containing intermediate, I_{nterm}, with which adsorbed hydrogen can react. Comparing the calculated rate constants for the processes, step (III) is clearly the rate-determining step in this reaction mechanism. Because hydrogen adsorption occurs on the platinum, it is likely that I_{nterm} is also located in the vicinity of these particles due to the fast reaction occurring on pulsing hydrogen, as shown in step (IV). Thus, step (III) may also include diffusion of adsorbed CO_2 to the active site for the reaction. The forward rate constant in step (III) for the formation of I_{nterm} was estimated from the exponential decay curve for CO production (Fig. 6). The reverse rate constant in step (III) was estimated from Fig. 7b. Step (V) is associated with desorption of CO from platinum [52]. Step (VI) is added to describe H_2O production from platinum to complete the reaction [53,54]. This mechanism does not include the second form of adsorbed CO_2 identified in the TAP experiments, because this decays on a time scale that is too long to be part of this reaction scheme.

$$CO_2 + \sigma \leftrightarrow CO_{2,ad}, \quad k_a = 170\ s^{-1},\ k_d = 1.3\ s^{-1}, \tag{I}$$

$$H_2 + 2Pt \leftrightarrow 2Pt\text{–}H, \quad k_a = 110\ s^{-1},\ k_d = 0.9\ s^{-1}, \tag{II}$$

$$CO_{2,ad} \leftrightarrow I_{nterm}, \quad \text{not fast, } k_f \approx 0.2\ s^{-1},\ k_b \approx 0.2\ s^{-1}, \tag{III}$$

$$I_{nterm} + Pt\text{–}H \leftrightarrow Pt\text{–}CO + OH_{ad}, \quad \text{fast, } k_b \approx 1.0\ s^{-1}\ [52], \tag{IV}$$

$$Pt\text{–}CO \leftrightarrow CO + Pt, \quad k_d \approx 1.5\ s^{-1}\ [52], \tag{V}$$

$$OH_{ad} + Pt\text{–}H \leftrightarrow H_2O + Pt + \sigma. \tag{VI}$$

Scheme 3.

Scheme 3 may be compared with Scheme 2 due to the fact that they are both associative mechanisms. There are a number of fundamental differences between the two schemes, however. In Scheme 2, adsorbed hydrogen reacts with adsorbed CO_2 to

form the formate intermediate; in comparison, in Scheme 3 the formation of the carbon-containing intermediate is slow and does not require the presence of adsorbed hydrogen on the surface. If adsorbed hydrogen were necessary, then a different dependence on the H_2 pulse time delay would be observed. Therefore, it is likely that the intermediate formed is not a simple formate species; it may be a surface carbonate. However, this is only a possibility, because the form of this carbon-containing intermediate cannot be directly identified from the TAP data. Subsequently, the reaction of this carbon-containing intermediate with adsorbed hydrogen is very fast, as shown in step (IV) of Scheme 3.

It should be noted that reaction Scheme 3 refers only to the associative pathway that dominates the CO yield under the conditions reported herein and does not exclude the high probability of other reaction pathways existing under different process conditions. The proposed mechanism provides a starting point for evaluating the possible contributions of redox and associative mechanisms for the WGS and RWGS reactions in future steady-state and transient studies taken over a range of temperatures and conditions.

The WGS/RWGS reaction is a challenge for TAP studies because of its global reversibility. However, using the large difference in the time scales of the separate steps and appropriate pulse sequences, it is possible to extract the various aspects of the mechanism and determine the rate constants of several elementary steps. To the best of our knowledge, the present work is the first paper to illustrate this property using the TAP technique [55].

4. Conclusion

The TAP technique was successfully applied for the first time to study RWGS reaction studies. The adsorption/desorption rate constants for CO_2 and H_2 were determined in separate TAP pulse-response experiments over reduced and CO_2-pretreated catalysts. In addition, the amount of H-containing active species was determined using D_2 multipulse TAP experiments. Remarkably, this number agrees with the amount of active sites observed in a previous SSITKA experiment. An associative reaction mechanism is thought to dominate for the fast RWGS reaction under TAP conditions, and a tentative reaction scheme has been proposed. The mechanism includes fast adsorption of CO_2 and H_2, slow formation of the CO_2 intermediate available for reaction, fast reaction of the CO_2 intermediate with adsorbed hydrogen, and release of adsorbed CO and water. In addition, a second species associated with CO_2 was found that desorbs on a time scale of minutes.

Acknowledgments

The authors thank Johnson Matthey for supplying the catalyst, the EPSRC (under the CARMAC project) for providing funding, and the Centre for Theory and Application of Catalysts (CenTACat) for providing a visiting research professorship to GSY.

References

[1] B.I. Whittington, C.J. Jiang, D.L. Trimm, Catal. Today 26 (1995) 41.
[2] J. Barbier Jr., D. Duprez, Appl. Catal. B 4 (1994) 105.
[3] T. Shido, Y. Iwasawa, J. Catal. 141 (1993) 71.
[4] J.T. Kummer, J. Phys. Chem. 90 (1986) 4747.
[5] E.C. Su, W.G. Rothschild, J. Catal. 99 (1986) 506.
[6] R.K. Hertz, J.A. Sell, J. Catal. 94 (1985) 166.
[7] K.C. Taylor, in: J.R. Anderson, M. Boudard (Eds.), Automobile Catalytic Converters, in: Catalysis: Science and Technology, vol. 5, Springer, Berlin, 1984.
[8] T. Bunluesin, R.J. Gorte, G.W. Raham, Appl. Catal. B 15 (1998) 107.
[9] J.M. Zalc, V. Sokolvskii, D.G. Löffler, J. Catal. 206 (2002) 169.
[10] S. Hilaire, X. Wang, T. Luo, R.J. Gorte, J. Wagner, Appl. Catal. A 215 (2001) 271.
[11] X. Wang, R.J. Gorte, Catal. Lett. 73 (2001) 15.
[12] Q. Fu, A. Weber, M. Flytzani-Stephanopoulos, Catal. Lett. 77 (2001) 87.
[13] T. Luo, R.J. Gorte, Catal. Lett. 85 (3–4) (2003) 139.
[14] X. Wang, R.J. Gorte, J.P. Wagner, J. Catal. 212 (2002) 225.
[15] G. Jacobs, P.M. Patterson, L. Williams, E. Chenu, D. Sparks, G. Thomas, B.H. Davis, Appl. Catal. A 262 (2004) 177.
[16] T. Tabakova, F. Boccuzzi, M. Manzoli, J.W. Sobczak, V. Idakiev, D. Andreeva, Appl. Catal. B 49 (2004) 73.
[17] G. Jacobs, E. Chenu, P.M. Patterson, L. Williams, D. Sparks, G. Thomas, B.H. Davis, Appl. Catal. A 258 (2004) 203.
[18] Y. Li, Q. Fu, M. Flytzani-Stephanopoulos, Appl. Catal. B 27 (2000) 179.
[19] G. Jacobs, S. Khalid, P.M. Patterson, D.E. Sparks, B.H. Davis, Appl. Catal. A 268 (2004) 255.
[20] T. Bunluesin, R.J. Gorte, G.W. Graham, Appl. Catal. B 14 (1997) 105.
[21] H. Cordatos, T. Bunluesin, J.S. Stubenrauch, J.M. Vohs, R.J. Gorte, J. Phys. Chem. 100 (1996) 785.
[22] D. Andreeva, T. Tabakova, V. Idakiev, D. Christov, R. Giovanoli, Appl. Catal. A 169 (1998) 9.
[23] V. Idakiev, T. Tabakova, Z.Y. Yuan, B.L. Su, Appl. Catal. A 270 (2004) 135.
[24] M. Haruta, Gold Bull. 37 (2004) 27.
[25] R.J. Gorte, S. Zhao, Catal. Today 104 (2005) 18.
[26] G. Jacobs, L. Williams, U. Graham, D. Sparks, B.H. Davis, J. Phys. Chem. B 107 (2003) 10398.
[27] G. Jacobs, E. Chenu, P.M. Patterson, L. Williams, D. Sparks, G. Thomas, B.H. Davis, Appl. Catal. A 258 (2004) 203.
[28] G. Jacobs, B.H. Davis, Appl. Catal. A 284 (2005) 31.
[29] G. Jacobs, A.C. Crawford, B.H. Davis, Catal. Lett. 100 (2005) 147.
[30] G. Jacobs, U.M. Graham, E. Chenu, P.M. Patterson, A. Dozier, B.H. Davis, J. Catal. 229 (2005) 499.
[31] G. Jacobs, P.A. Patterson, U.M. Graham, D.E. Sparks, B.H. Davis, Appl. Catal. A 269 (2004) 63.
[32] Q. Fu, H. Saltsburg, M. Flytzani-Stephanopoulos, Science 301 (2003) 935.
[33] Q. Fu, W. Deng, H. Saltsburg, M. Flytzani-Stephanopoulos, Appl. Catal. B 56 (2005) 57.
[34] Q. Fu, S. Kudriavtseva, H. Saltsburg, M. Flytzani-Stephanopoulos, Chem. Eng. J. 93 (2003) 41.
[35] S. Golunski, R. Rajaram, N. Hodge, G.J. Hutchings, C.J. Kiely, Catal. Today 72 (2002) 107.
[36] J.C. Frost, Nature 334 (1988) 577.
[37] A. Amieiro Foncesca, R. Burch, Y. Chen, J. Fisher, A. Goguet, C. Hardacre, P. Hu, D. Thompsett, D. Tibiletti, J. Phys. Chem. B, submitted for publication.
[38] A. Goguet, F. Meunier, J.P. Breen, R. Burch, M.I. Petch, A. Faur Ghenciu, J. Catal. 226 (2004) 382.
[39] D. Tibiletti, A. Goguet, F.C. Meunier, J.P. Breen, R. Burch, Chem. Commun. (2004) 1636.
[40] A. Goguet, D. Tibiletti, F.C. Meunier, J.P. Breen, R. Burch, J. Phys. Chem. B 108 (2004) 20240.
[41] F.C. Meunier, D. Reid, S. Shekhtman, D. Tibiletti, A. Goguet, C. Hardacre, R. Burch, unpublished results.
[42] J.T. Gleaves, J.R. Ebner, T.C. Kuechler, Catal. Rev. Sci. Eng. 30 (1988) 49.

[43] J.T. Gleaves, G.S. Yablonsky, P. Phanawadee, Y. Schuurman, Appl. Catal. A 160 (1997) 55.
[44] G.S. Yablonsky, M. Olea, G.B. Marin, J. Catal. 216 (2003) 120.
[45] S.O. Shekhtman, G.S. Yablonsky, J.T. Gleaves, R. Fushimi, Chem. Eng. Sci. 58 (2003) 4843.
[46] S. Bernal, F.J. Botana, J.J. Calvino, M.A. Cauqui, G.A. Jobacho, J.M. Pintado, J.M. Rodriguez-Izquierdo, J. Phys. Chem. 97 (1993) 4118.
[47] S.O. Shekhtman, G.S. Yablonsky, J.T. Gleaves, S. Chen, Chem. Eng. Sci. 54 (1999) 4371.
[48] P. Phanawadee, S.O. Shekhtman, C. Jarungmanorom, G.S. Yablonsky, J.T. Gleaves, Chem. Eng. Sci. 58 (2003) 2215.
[49] S.O. Shekhtman, G.S. Yablonsky, J.T. Gleaves, R. Fushimi, Chem. Eng. Sci. 59 (2004) 5493.
[50] S.O. Shekhtman, G.S. Yablonsky, Ind. Eng. Chem. Res. 44 (2005) 6518.
[51] S.O. Shekhtman, G.S. Yablonsky, paper in preparation.
[52] S.O. Shekhtman, A. Goguet, C. Hardacre, F.C. Meunier, R. Burch, G.S. Yablonsky, in preparation.
[53] K. Beduerfig, S. Voelkening, Y. Wang, J. Winterllin, K. Yacobi, G. Ertl, J. Chem. Phys. 111 (24) (1999) 11147.
[54] A. Norman, V. Perrichon, Phys. Chem. Chem. Phys. 5 (2003) 3557.
[55] TAP Workshop, 6–8 December 2004, Leipzig, Germany.